Residual dust charges in discharge afterglow

L. Couëdel,* M. Mikikian, and L. Boufendi
GREMI (Groupe de Recherches sur l'Énergétique des Milieux Ionisés), CNRS/Université d'Orléans, 14 rue d'Issoudun, 45067 Orléans Cedex 2, France

A. A. Samarian
School of Physics A28, University of Sydney, NSW 2006, Australia
(Received 24 May 2006; published 22 August 2006)

An on-ground measurement of dust-particle residual charges in the afterglow of a dusty plasma was performed in a rf discharge. An upward thermophoretic force was used to balance the gravitational force. It was found that positively charged, negatively charged, and neutral dust particles coexisted for more than 1 min after the discharge was switched off. The mean residual charge for 200-nm-radius particles was measured. The dust particle mean charge is about $-5e$ at a pressure of 1.2 mbar and about $-3e$ at a pressure of 0.4 mbar.

DOI: 10.1103/PhysRevE.74.026403 PACS number(s): 52.27.Lw

I. INTRODUCTION

Dusty or complex plasmas are partially ionized gas composed of neutral species, ions, electrons, and charged dust particles. In laboratory experiments, these particles can be either injected or grown directly in the plasma. Injected dust particles are usually micron-size particles. Due to their mass, they are confined near the bottom electrode where the electric force counterbalances gravity. The microgravity condition is necessary to study dust clouds of micrometer-size particles filling the whole plasma chamber [1]. In the laboratory, dense clouds of submicron particles light enough to completely fill the gap between the electrodes can be obtained using reactive gases such as silane [2,3] or using a target sputtered with ions from plasma [4–7].

Dust-particle charge is a key parameter in complex plasma. It determines the interaction between a dust particle and electrons, ions, its neighboring dust particles, and electric field. The determination of the dust-particle charge is thus one of the basic problems in any complex plasma experiments. Knowledge of dust charge will allow us to understand the basic properties of dusty plasma, particle dynamics in dust clouds, and methods to manipulate the particles.

The particle charge controls the dust dynamics both in laboratory and technological plasma reactors, and also in space plasmas. Thus one of the main dusty plasma challenges is to understand the dust charging in a wide range of experimental conditions, which simulates industrial and space plasmas. For example, in most industrial processes in the microelectronics industry which uses silane as the reactive gas, dust contamination is a vital problem [8]. The dust dynamics and coagulation in space plasma are also phenomena governed by dust-particle charges [9,10].

There are many publications reporting on the investigation of dust charging in discharge plasma; see [11–18] and references therein. However there are only a few papers devoted to dust charging, or decharging to be more specific, in the discharge afterglow. In [19] a diffusion of fine dust particles (8–50 nm) in the afterglow of a dusty plasma has been studied. From the afterglow decay of dust number density the charged fraction of particles has been measured. It was found that some particles carried a very small residual charge and some were neutral. A model has been proposed to explain charges on particles in the late afterglow of a dusty plasma. An observation of decay, or "decharging," of an rf plasma with dust particles after switching off the discharge power was reported in [20]. Experiments were performed in the PKE-Nefedov reactor [1] under microgravity conditions on board the International Space Station. The existence of negative residual charges has been shown. A simple theoretical model that describes data obtained was proposed. The residual charges were attributed to the presence of an excitation electric field that was used for dust charge measurements. The limitations of the Space Station experiment routine could not prove this hypothesis. Theoretical predictions on an effect of rf plasma parameters on residual charges has also not been verified.

So any new experimental evidence of residual dust charges in afterglow plasma will lead to a better understanding in the decharging of complex plasma. Indeed the value and nature of residual charges after plasma extinction is of great importance. The dust-particle charge in afterglow plasma could induce a problem in future single-electron devices where a residual charge attached on deposited nanocrystals would be the origin of dysfunction. It could make easier industrial plasma processing reactor decontamination thanks to the use of specially designed electric fields. The residual charges on dust particles in fusion reactors (such as ITER) also can make the cleaning process much easier.

In this paper, we report an on-ground experiment on the residual charge measurement of dust particles after the decay of a dusty plasma. The experiment was performed in the PKE-Nefedov reactor where the dust particles were physically grown in the plasma. A temperature gradient was introduced in the chamber to create an upward thermophoretic force to balance gravity. The residual charges were determined from an analysis of dust oscillations, which were excited by applying a sinusoidal bias to the bottom electrode. A coexistence of positively and negatively charged dust par-

*Electronic address: lenaic.couedel@univ-orleans.fr

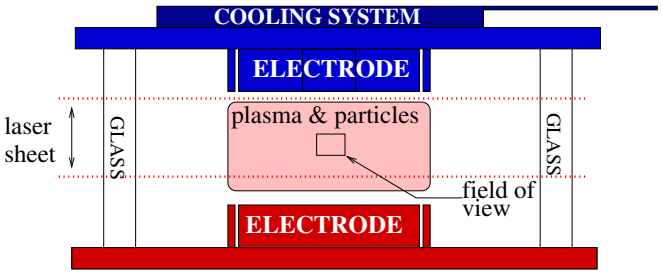

FIG. 1. (Color online) Schematic of the experimental apparatus.

ticles as well as noncharged ones was found for more than 1 min after the discharge was switched off. The residual charges for 200-nm-radius particles have been measured for two different pressures. It was revealed that dust particles kept the residual charges only when the discharge was abruptly switched off. In the case when the discharge power is decreased slowly until the plasma disappeared, there was no residual charge on the dust particles. It was also shown that the presence of the low-frequency excitation electric field did not play any role in keeping the charge on dust particles in the afterglow plasma.

The article is organized as follows. Section II is devoted to a general description of the experimental setup. In Sec. III we analyze the forces acting on dust particles, paying most attention to the thermophoretic force. In Sec. IV we discuss a procedure of residual charge measurement and present experimental data obtained, and in Sec. V we analyze discharging of dust particle in afterglow plasma. Section VI is the conclusion.

II. EXPERIMENTAL SETUP

The work presented here is performed in the PKE-Nefedov (Plasma Kristall Experiment) chamber designed for microgravity experiments [1]. It is an rf discharge operating in push-pull excitation mode. It consists of 4-cm-diam parallel electrodes separated by 3 cm. The injected power varies in the range 0–4 W. Dust particles are grown in an argon plasma (0.2–2 mbar) from a sputtered polymer layer deposited on the electrodes and coming from previously injected dust particles (3.4 μm, melamine formaldehyde). A detailed description of this experiment and previous results are presented in Refs. [1,4,5].

For the study concerning residual charges, the top electrode was cooled (Fig. 1). An upward thermophoretic force was applied to dust particles in order to counterbalance gravity [21] when the plasma is off. To study particle charges, a sinusoidal voltage produced by a function generator with amplitude ±30 V and frequency of 1 Hz was applied to the bottom electrode. The induced low-frequency sinusoidal electric field $\boldsymbol{E}(\boldsymbol{r},t)$ generated dust oscillations if they kept a residual electric charge.

A thin laser sheet perpendicular to the electrodes illuminates dust particles and the scattered light is recorded at 90° with standard charge coupled device (CCD) cameras with 25 images per second. Video signals were transferred to a computer via a frame-grabber card with 8-bit gray scale and 560×700 pixel resolution. In order to avoid edge effect, a field of view over 8.53×5.50 mm^2 restrained to the center of the chamber was used for residual charge measurement. By superimposition of video frames particle trajectories have been obtained. The coordinates of the particles were measured in each third frame. The amplitude of the oscillations was figured out from the measured particle positions. Absolute values for the oscillation amplitude were obtained by scaling the picture pixels to the known size of the field of view.

III. FORCES ACTING ON DUST PARTICLES

Dust particles in laboratory plasmas are subjected to various forces that confine them in the plasma or drag them out (to the walls or pump outlet) [8]: the confining electrostatic force, the gravity, the thermophoretic force, the ion drag force, and the neutral drag force.

After the discharge is switched off, the forces still acting on dust particles are the gravity F_g, the thermophoretic force F_T, the neutral drag force F_{dn}, and, if dust particles keep residual charges, the electric force F_E due to the electric field induced by the sinusoidal voltage applied to the lower electrode. In this experiment the thermophoretic force balanced the gravity force and the electrostatic force was the reason for the dust oscillations while the neutral drag force dampens the last ones.

The expression for the gravity force is

$$\boldsymbol{F}_g = \frac{4}{3}\pi r_d^3 \rho \boldsymbol{g}, \tag{1}$$

where $\boldsymbol{g}$ is the gravity acceleration, r_d the dust particle radius, and ρ its mass density.

The neutral drag force was taken as [22]

$$\boldsymbol{F}_{dn} = -\frac{8}{3}\sqrt{2\pi} r_d^2 m_n n_n v_{Tn}\left(1+\alpha_{ac}\frac{\pi}{8}\right)(\mathbf{v}_d - \mathbf{v}_n), \tag{2}$$

where m_n is the neutral atom mass, n_n the neutral atom density, $v_{Tn}=\sqrt{8k_BT_n/\pi m_n}$ the thermal speed with $T_n=T$ the neutral gas temperature, k_B the Boltzmann constant, α_{ac} the accommodation coefficient, $\mathbf{v}_d$ dust particle speed, and $\mathbf{v}_n$ a mean speed of neutral atoms. In our experiment $\mathbf{v}_n$ can be taken as 0 because there is no gas flow.

The electric force can be written as

$$\boldsymbol{F}_E(\boldsymbol{r},t) = Q_d \boldsymbol{E}(\boldsymbol{r},t), \tag{3}$$

where Q_d is the dust particle electric charge and $\boldsymbol{E}(\boldsymbol{r},t)$ is the electric field between the electrodes after the plasma is switched off. In the late afterglow the plasma density is very small and $\boldsymbol{E}(\boldsymbol{r},t)$ can be approximated by the vacuum field above a charged disk. Taking into account the size of the camera field of view, the size of the electrode, and the fact that camera was directed to the region near center of the chamber, we are interested in the electric field vertical component $\boldsymbol{E}(\boldsymbol{r},t)\approx E_z(z,t)\vec{e}_z \equiv E(z,t)\vec{e}_z$ only. The calculated value of $E(z,t)$ at the central axis is presented in Fig. 2.

The expression for the thermophoretic force must be chosen carefully. Indeed, it depends strongly on the Knudsen

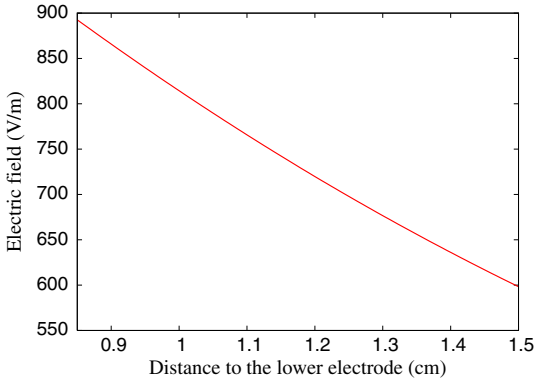

FIG. 2. (Color online) Vertical component of the electric field in the camera field of view.

number $\mathrm{Kn}=l/r_d$ [23] where l is the mean free path of buffer gas species. In our experiment, we work at an operating pressure around 1 mbar. In a previous paper [4], the size of grown dust particles was reported between 200 nm and 800 nm. It gives, using results from Varney [24] for an atom-atom cross section, Knudsen number $250<\mathrm{Kn}<1000$. Consequently we operate in a free molecular regime where a dust particle is similar to a very large molecule. Many theories have been developed [23,25–28] and used [21,23,29] for thermophoresis in the free molecular regime. The most commonly used equation is the Waldmann equation [28] which has been verified experimentally [30,31]:

$$\boldsymbol{F}_T = -\frac{32}{15} r_d^2 \frac{k_{tr}}{v_{Tn}} \boldsymbol{\nabla} T, \tag{4}$$

where $\boldsymbol{\nabla} T$ is the temperature gradient in the gas and k_{tr} the translational part of the thermal conductivity given for a monoatomic gas by [32]

$$k_{tr} = \frac{15 k_B}{4 m_n} \mu_{ref} \left(\frac{T}{T_{ref}} \right)^{\nu}, \tag{5}$$

where μ_{ref} is the reference viscosity at reference temperature $T_{ref}=273$ K and the exponent ν results from a best fit of experimental viscosity near the reference temperature. For argon, $\mu_{ref}=2.117\times10^{-5}$ Pa s and $\nu=0.81$ [32].

Another important effect that must be considered in the estimation of thermophoretic force is the influence of a finite volume of gas. If the pressure is low enough, the gas mean free path can become comparable to a length scale of experimental apparatus and the gas can no longer be treated as a continuous medium. Under such a condition, an additional Knudsen number must be added [23], $\mathrm{Kn}_L=l/L$, where L is the length scale of the reactor. In this experiment, the length between electrodes is $L=3$ cm giving $\mathrm{Kn}_L\sim5\times10^{-3}$ which means the gas can be considered as a continuous medium.

The temperature gradient between the electrodes was calculated with FEMLAB (steady-state analysis of heat transfer through convection and conduction with heat flux, convective and temperature boundary conditions using the Lagrange-Quadratic element). The temperatures on the electrodes were measured by a thermocouple and used as boundary conditions for the problem. The contour plot obtained is

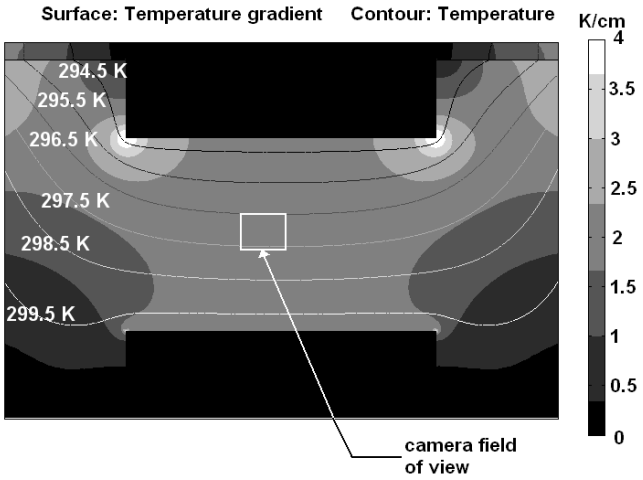

FIG. 3. Temperature profile and gradient.

presented in Fig. 3. It shows that the vertical component of the temperature gradient is constant near the reactor center. The value of temperature gradient is about 2 K/cm for our experiment. There is also a small horizontal component of the temperature gradient. This is the reason for particle drift in the horizontal direction. Such a drift allowed us to resolve particle trajectories (see next section) and made particle charge measurement more convenient.

IV. EXPERIMENTAL PROCEDURE AND RESULTS

In this section, dust-particle size estimation and residual charge measurement are presented. The residual charge measurements have been performed by the following routine. First the chamber was pumped down to lowest possible pressure (base pressure $\sim2\times10^{-6}$ mbar) and the cooling system was turned on. After this, argon was injected up to the operating pressure, the discharge was started, and particles were grown, forming familiar structures such as a void (see, for example, [5]). Then, the discharge was switched off and the bottom electrode was biased by sinusoidal voltage.

In afterglow plasma, the dynamics of dust particles is determined by a temperature gradient and excitation electric field. Figure 4 presents a superimposition of images taken after discharge had been switched off. There are two different types of motion observable. Dust particles drift upwards, downwards, and to the side due to existing temperature gradients and they oscillate due to electrostatic force. It is obvious that the thermophoretic force acts on any dust particle in the chamber, while the electrostatic force acts only if particles have charge in afterglow. Thus the presence of oscillating particles (see Fig. 4) clearly indicates that dust particles do have residual charges after the discharge has been switched off. Dust particles oscillating in opposite phases as well as nonoscillating dust grains have been observed, indicating that negatively charged, positively charged, and noncharged dust particles coexist after plasma extinction. It is worth mentioning that in order to observe dust oscillations the discharge must be switched off abruptly. It was shown that if the power was decreased slowly until the plasma dis-

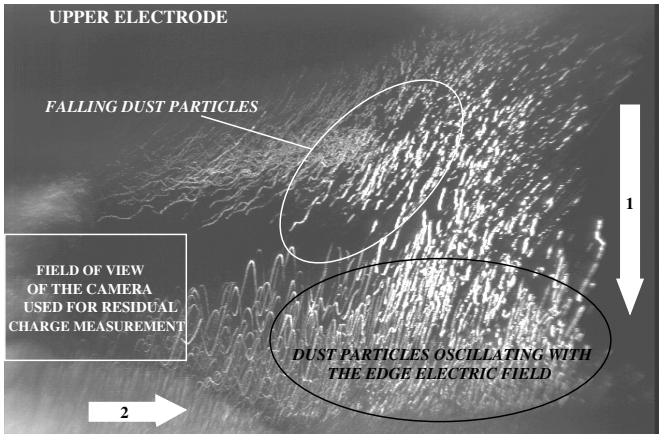

FIG. 4. Superimposition of video frames taken with a large-field-of-view CCD camera. Arrows 1 and 2 represent, respectively, the vertical and horizontal components of the temperature gradient. Edge effects as well as falling dust particles can be seen.

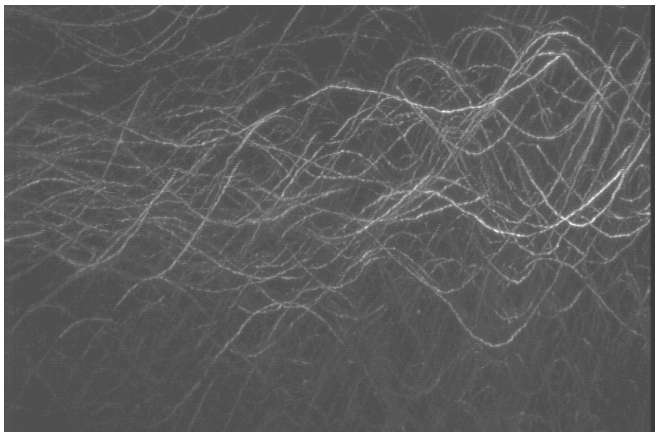

FIG. 5. Superimposition of video frames 10 s after plasma extinction. Dust-particle oscillations can clearly be seen. The temperature gradient has a slight horizontal component. Therefore, oscillations are in the two-dimensional laser plane.

appears, there are no residual charges (no oscillations of dust particles in the sinusoidal electric field were observed). Another interesting fact is that the residual charge on dust particles has a long relaxation time and does not depend on time when the excitation electric field was applied. Dust oscillations were observed for more than 1 min after plasma extinction and in both cases when the function generator was switched on during the discharge or a few seconds after the discharge is turned off.

As can be seen in Fig. 4, there are dust particles falling after the discharge is switched off. These particles are too big to be sustained by the thermophoretic force. Other particles are horizontally adrift at constant height; this means that for these particles the gravity force is balanced by the thermophoretic force. These particles have been used to measure residual charges. It is clear from Fig. 4 that use of a large-field-of-view camera gives us a nice overall picture of decaying dusty plasma but it is not suitable for residual charge measurement because edge effects cannot be neglected. Thus a camera with a small field of view was used for the charge measurement (see Fig. 4). The superimposition of images from this camera is presented in Fig. 5. These images give us a clear track of the dust oscillations, so dust grain trajectories can be reconstructed (Fig. 6).

A. Size and mass of levitating dust grains in discharge afterglow

Particle size (mass) and residual charge measurement are strongly related in this experiment. Charge, size, and mass of dust particles have to be determined. Considering that dust particles levitating in a reactor at a constant height after plasma extinction are the ones for which the gravity is exactly balanced by the thermophoretic force, the dust particle radius can be found using Eqs. (1) and (4):

$$r_d = -\frac{8}{5\pi\rho g}\frac{k_{tr}}{v_{th}}\nabla T. \tag{6}$$

Dust grains are supposed to be spherical and mainly made of carbon (sputtering of a carbonaceous polymer material) [4] so that the mass m_d can be deduced from Eq. (6):

$$m_d = \frac{4}{3}\pi r_d^3 \rho, \tag{7}$$

where ρ is the mass density of graphite. In our experimental condition, the radius of levitating dust grains is estimated to $r_d \simeq 190$ nm and their mass is $m_d \simeq 6.5 \times 10^{-17}$ kg.

B. Dust-charge measurement

From the measurement of oscillation amplitude, the residual charge on a dust particle can be obtained. As the gravity is compensated by the thermophoretic force, the equation of motion for one dust particle, neglecting its interactions with other dust particles, can be reduced to

$$m_d \ddot{z} = F_E(z,t) + F_{nd}(\dot{z}). \tag{8}$$

Taking $E(t)=E_0(z_{mean})\cos(\omega t)$ (the amplitude of the electric field E_0 is the one at the mean dust levitation height z_{mean}) and using Eqs. (3), (2), and (8), the dust-particle oscillation amplitude b can be obtained [33]:

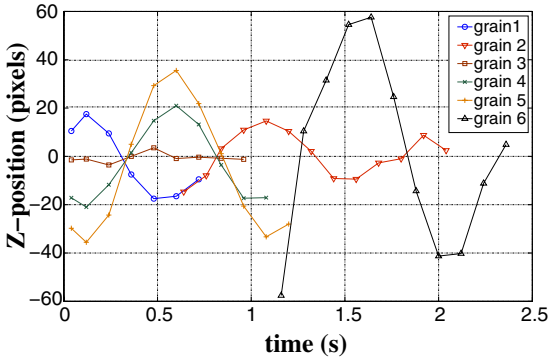

FIG. 6. (Color online) Oscillation of six dust grains 10 s after plasma extinction. Nonoscillating dust grains and opposite phase oscillations are observed.

TABLE I. Measured maximum, minimum, and mean dust-particle residual charges for the two operating pressures.

	$P=1.2$ mbar	$P=0.4$ mbar
∇T	-190 K m^{-1}	-177 K m^{-1}
r_d	194 nm	180 nm
m_d	6.9×10^{-17} kg	5.4×10^{-17} kg
γ	1.36×10^{-13} kg s^{-1}	0.39×10^{-13} kg s^{-1}
$Q_{d_{res}max}$	$+2e$	$+2e$
$Q_{d_{res}min}$	$-12e$	$-4e$
$Q_{d_{res}mean}$	$-5e$	$-3e$

$$b(\omega,Q_d,E_0)=\frac{Q_dE_0(z_{mean})}{m_d\omega\sqrt{\omega^2+4\gamma^2/m_d^2}}, \tag{9}$$

where $\gamma=(4/3)\sqrt{2\pi}r_d^2m_nn_nv_{Tn}[1+\alpha_{ac}(\pi/8)]$ is the damping coefficient and $\omega=2\pi f$ where f is the frequency imposed by the function generator. Equation (9) can easily be inversed to derive the dust residual charge:

$$Q_{d_{res}}=\frac{m_db(\omega,Q_d,E_0(z_{mean}))\omega\sqrt{\omega^2+4\gamma^2/m_d^2}}{E_0(z_{mean})}. \tag{10}$$

The sign of the dust-particle charge is deduced from the phase of the dust-particle oscillation with respect to the excitation electric field. Oscillation amplitudes up to 1.1 mm have been measured (depending on the operating pressure) and charges from $-12e$ to $+2e$ are deduced where e is the elementary charge. It has been found that at high pressure dust particles keep a higher mean residual charge (Table I) but uncertainties are of $\sim 2e$ for each measurement.

V. DISCUSSION

The charging (discharging) process of dust particles in a plasma is governed by the contributions of all currents entering (or leaving) the dust surface, involving plasma electrons and ion currents, photoemission and thermionic emission currents, etc.

$$\frac{dQ_d}{dt}=\sum I_a+\sum I_l, \tag{11}$$

where I_a and I_l are currents absorbed and emitted by the particle (with appropriate sign). In most cases for discharge plasmas we can ignore the emission current and the kinetics of the particle charge can be expressed as

$$\frac{dQ_d}{dt}=J_i-J_e=-\pi er_d^2[n_ev_{T_e}e^{-\varphi}-n_iv_{T_i}(1+\tilde{T}_e\varphi)], \tag{12}$$

where J_e and J_i are the fluxes of electrons and ions onto the particle, $v_{T_{i(e)}}=\sqrt{8k_BT_{i(e)}/\pi m_{i(e)}}$ the thermal velocity of ions (electrons), $\tilde{T}_e=T_e/T_i$ is the electron to ion temperature ratio, $n_{i(e)}$ is the density of ions (electrons), and $\varphi=-eQ_d/4\pi\epsilon_0k_Br_dT_e$ is the dimensionless surface potential of a dust particle where ϵ_0 is the vacuum dielectric permittivity. According to Eq. (12), charge on a dust particle depends on the electron-ion masses, temperatures, and density ratios m_e/m_i, n_e/n_i, and T_e/T_i. Thus to analyze the decharging of dust particle in afterglow plasma one needs to consider the kinetics of plasma decay.

The plasma diffusion loss and electron temperature relaxation determine the kinetics of the discharge plasma decay [34]. In the presence of dust particles, plasma loss is due to diffusion onto the walls completed by surface recombination on dust particles. The equations for the plasma density and electron temperature relaxation are [34,35]

$$\frac{d\tilde{n}}{dt}=-\frac{\tilde{n}}{\tau_L}, \tag{13}$$

$$\frac{d\tilde{T}_e}{dt}=-\frac{\tilde{T}_e-1}{\tau_T}, \tag{14}$$

where $\tilde{n}=n_{i,e}/n_0$ with n_0 the initial plasma density, τ_L the time scale of the plasma loss, and τ_T the time scale for electron temperature relaxation. The expressions for the time scales are [34,35]

$$\tau_L^{-1}=\tau_D^{-1}+\tau_A^{-1}, \tag{15}$$

$$\tau_D^{-1}\simeq\frac{l_{in}v_{T_i}}{3\Lambda^2}(1+\tilde{T}_e)\equiv\frac{1}{2}(1+\tilde{T}_e)\frac{1}{\tau_D^\infty}, \tag{16}$$

$$\tau_A^{-1}\simeq\pi r_d^2n_dv_{T_i}(1+\varphi\tilde{T}_e)\equiv\left(\frac{1+\varphi\tilde{T}_e}{1+\varphi}\right)\frac{1}{\tau_A^\infty}, \tag{17}$$

$$\tau_T^{-1}=\sqrt{\frac{\pi}{2}}\sqrt{\frac{m_e}{m_i}}\frac{v_{T_i}}{l_{en}}\sqrt{\tilde{T}_e}\equiv\frac{\sqrt{T_e}}{\tau_T^\infty}, \tag{18}$$

where τ_D is the ambipolar diffusion time scale onto the walls, τ_A the particle absorption time scale, $l_{i(e)n}$ the mean free path of the ion- (electron-) neutral collision, and Λ the characteristic diffusion length ($\Lambda\sim1$ cm in this experiment). The ∞ exponent stands for the limit at very long time.

For a charging time scale lower than the plasma decay or temperature relaxation time scales the charge on the dust particle is in equilibrium—i.e., ion and electron fluxes balance each other—$\varphi\simeq\varphi_{eq}$, and using Eq. (12), φ_{eq} is given by

$$\frac{n_e}{n_i}\sqrt{\tilde{T}_e}e^{-\varphi_{eq}}=\sqrt{\frac{m_e}{m_i}}(1+\tilde{T}_e\varphi_{eq}). \tag{19}$$

In this case, the expressions for the charge fluctuation and charge fluctuation time scale τ_Q are

$$\frac{dQ_d}{dt}\simeq-\frac{Q_d-Q_{deq}}{\tau_Q}, \tag{20}$$

$$\tau_Q^{-1}\simeq\frac{v_{T_i}r_d}{4\lambda_{i0}^2}(1+\varphi_{eq})\tilde{n}\equiv\frac{\tilde{n}}{\tau_Q^0}, \tag{21}$$

where $\lambda_{i0}=\sqrt{\epsilon_0k_BT_i/n_0e^2}$ is the initial ion Debye length.

It should be noted that the time scale for dust charge fluctuations strongly depends on the plasma density and can

TABLE II. Values of the different time scales for the two operating pressures.

	$P=0.4$ mbar	$P=1.2$ mbar
τ_D^0	30 μs	90 μs
τ_D^∞	1.5 ms	5 ms
τ_A^0	0.4 ms	0.4 ms
τ_A^∞	30 ms	30 ms
τ_L^0	30 μs	90 μs
τ_L^∞	1.4 ms	4.3 ms
τ_T^0	100 μs	34 μs
τ_T^∞	1 ms	340 μs
τ_Q^0	4 μs	4 μs
t_c	20 ms	60 ms
$\tau_Q(t_c)$	1.4 s	1.4 s

vary from microseconds for the initial stages of plasma decay up to seconds in the case of almost extinguished plasma. Taking into account Eqs. (13) and (21), the time dependence of τ_Q can be expressed as [20]

$$\tau_Q^{-1} = \frac{1}{\tau_Q^0} \exp(-t/\tau_L). \tag{22}$$

To understand the dusty plasma decharging dynamics we have to compare different time scales. In Table II, the time scales for this experiment are presented. It can be seen that the initial charge fluctuation time scale is the shortest. The temperature relaxation time scale is shorter or becomes comparable (for 0.4 mbar) to the plasma density decay time scale and plasma losses mainly determined by diffusion. The latest means that for our experimental conditions dust particles did not affect the plasma decay at the initial stage. Figure 7 presents the qualitative dependence of the main plasma and dust particle parameters during the afterglow. Four stages of the dust plasma decay can be labeled. As we can see, the first stage of the plasma decay ($t<\tau_T$) is characterized by the electron temperature T_e drop down to room temperature, while the plasma density (especially in case $\tau_T^0<\tau_L^0$) is slightly decreased. As the charging time scale is almost independent of $\tilde{T}_e$ [Eq. (21)], the charge is still determined by its equilibrium value [Eq. (12)]. During the temperature relaxation stage the particle charge should decrease to the value [20]

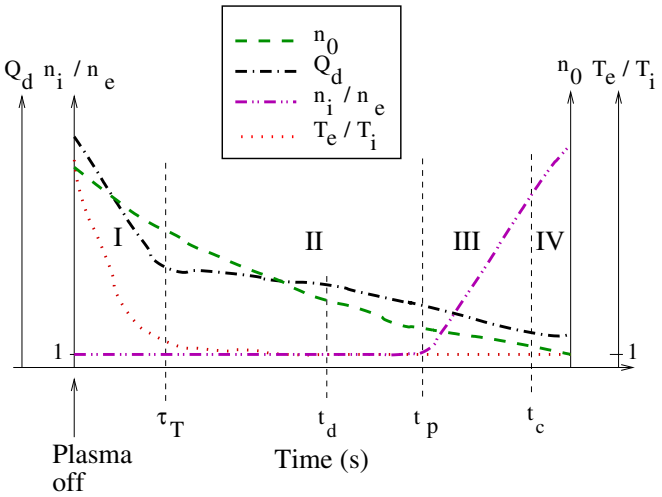

FIG. 7. (Color online) Qualitative time evolution of dust charge, plasma density, and electron temperature during the afterglow. Four stages of the dust plasma decay can be identified: I: temperature relaxation stage up to t_T. II: plasma density decay stage up t_p. III: dust charge volume stage t_c. IV: frozen stage.

$$Q_{rT} = \frac{1}{\tilde{T}_{e0}} \left(\frac{\varphi_{eq}(1)}{\varphi_{eq}(\tilde{T}_{e0})} \right) Q_0 \simeq \frac{Q_0}{62} \simeq -15e, \tag{23}$$

where Q_0 is the initial dust charge in the plasma and Q_{rT} the value of the dust residual charge at the end of the first decay stage. The dust charge in the plasma Q_0 was estimated as $Q_0=-950e$, solving numerically Eq. (19), with the given parameters $T_i=300$ K and $T_e\simeq 3$ eV, for argon plasma with $n_i\cong n_e$. At the next stage of decay, the electron temperature is stabilized while the plasma density is still decreasing (see Fig. 7). So τ_Q continues increasing according to Eqs. (12) and (21). When τ_Q becomes comparable to τ_L, the particle charge cannot be considered as in equilibrium and to determine particle charge we should use Eq. (12). The time scale when the particle charge starts sufficiently deviating from the equilibrium can be estimated as [Eqs. (15) and (22)]

$$t_d \sim -\tau_L^\infty \ln\left[\frac{8}{3} \left(\frac{\lambda_{i0}}{\Lambda} \right)^2 \frac{l_{in}}{r_d} \right] \sim 6\tau_L^\infty. \tag{24}$$

However, according to Eq. (12), as long as the plasma is neutral ($n_e=n_i$) the charge on the dust particle does not change. The plasma will keep quasineutrality until decaying rates for the electrons and ions are the same. It will be true in the case of ambipolar diffusion. When the nature of the diffusion changes, electrons and ions start to diffuse independently, which will lead to a changing n_e/n_i ratio and consequently the dust charge change.

The nature of the plasma diffusion changed when the particle volume charge cannot be ignored or when the plasma screening length becomes comparable to the chamber size. In the first case the ion diffusion will be influenced by the negatively charged dust particles, while the electrons will be free to go. In the second case, large density differences appear over distances less than the screening length and electrons and ions diffuse independently. Let us estimate the characteristic times for both cases.

The influence of the overall particle charge is determined by the value of the Havnes parameter $P_e=-NQ_d/en_e$. Based on the model discussed, the qualitative evolution of the Havnes parameter P_e in dusty plasma afterglow can be plotted as shown in Fig. 8. The initial value of P_e is small ($\sim$0.06 with an estimated dust density $N\sim 2\times 10^5$ cm^{-3} and $n_0\simeq n_{e0}\sim 5\times 10^9$ cm^{-3}) and there is no influence of dust. At the first stage of decaying (temperature relaxation stage) P_e decreases due to a dramatic decrease of the dust charge while the plasma density decreases by a factor of 1.1. At τ_T, P_e reaches its minimum value of about 1×10^{-3}. After this P_e starts increasing. During this stage the dust particle charge

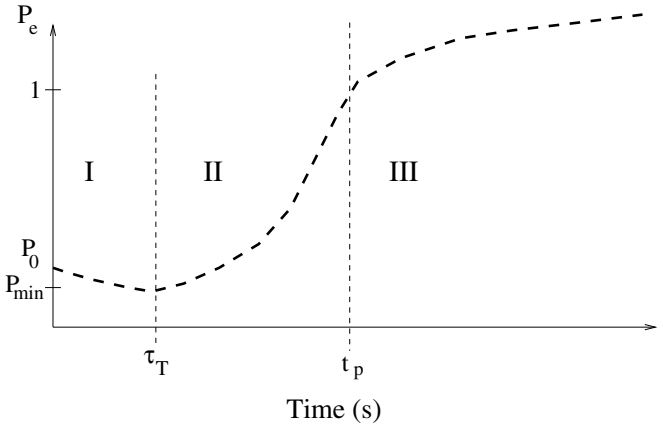

FIG. 8. Qualitative time evolution of the Havnes parameter after the power is switched off.

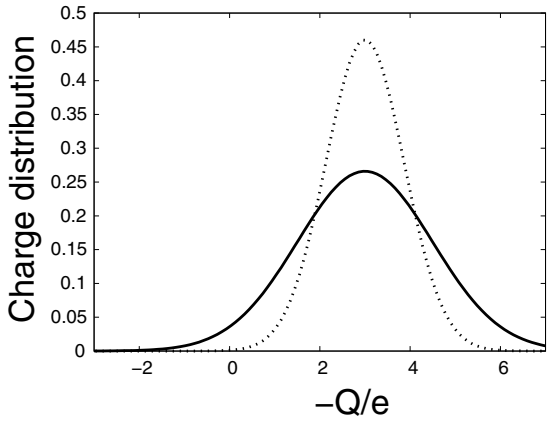

FIG. 9. Charge distribution with and without image force correction. The dotted line represents the distribution with $\Delta Q=0.5\sqrt{Q}$. The solid line represents the distribution with $\Delta Q=0.87\sqrt{Q}$ [37].

changes slowly while the plasma number density decays fast (see Fig. 7). The time at which P_e becomes ~ 1 can be estimated as [Eqs. (13)–(18)]

$$t_p \sim \tau_L^{\infty} \ln\left[\left(\frac{T_{e0}}{T_n}\right)\left(\frac{-en_0}{Q_d N}\right)\right] \sim 8\tau_L^{\infty}. \tag{25}$$

The screening length becomes comparable to the chamber size—i.e., $\lambda_i(\tilde{n}_c)\sim\Lambda$—when the density drops down to $\tilde{n}_c=\lambda_{i0}^2/\Lambda^2$. This occurs at [20]

$$t_c \sim \tau_L^{\infty} \ln \tilde{n}_c^{-1} \sim 10\tau_L^{\infty}. \tag{26}$$

At time $\min[t_p,t_c]$, electrons start running away faster than ions and the ratio n_i/n_e grows. For our experimental conditions $t_p<t_c$; thus, the neutrality violation due to the presence of dust particles happens before the Debye length exceeds the chamber size. So the third stage of dusty plasma decay starts at t_p. During this stage the charge on the dust particles is changed due to the changing of the n_e/n_i ratio. At this stage $t_d<t_p$, thus, the kinetic equation (12) should be used for estimations of the charge variation. The upper limit of the charge change can be estimated ignoring the electron current and considering the time interval between t_p and t_c,

$$\frac{dQ}{dt} < J_i\Big|_{t_p}^{t_c} \tag{27}$$

$$< \pi e r_d^2 n_i(t_p) v_{T_i} \left(1 - \frac{e}{4\pi\epsilon_0 k_B r_d T_i} Q_d\right)\Big|_{t_p}^{t_c}. \tag{28}$$

Solving Eq. (28), the charge should evolve as follows:

$$Q_d = \left(Q_{dT} - \frac{1}{\alpha}\right)\exp(-K\alpha\Delta t) + \frac{1}{\alpha}, \tag{29}$$

where $\alpha=e/4\pi\epsilon_0 k_B r_d T_i \sim 0.28/e$, $K=\pi e r_d^2 n_i(t_p) v_{T_i} \sim 190e$, and thus $(K\alpha)^{-1}\sim 20$ ms $\sim \Delta t=(t_c-t_p)$.

Therefore, the charge during the third stage decreases to $-3e$. At the fourth stage of plasma decay, $t>t_c$, the plasma density decreases such that any further changes of the dust charge become negligible and the charge remains constant for a while. Thus the final residual charge for our condition is expected to be about $Q_{d_{res}}\sim -3e$ which is well correlated with the charges measured in the experiment (Table I).

The observation of neutral and positively charged particles in our experiments can be explained by the particle charge distribution. The charge distribution in a dust-particle ensemble is due to charge fluctuation on every individual dust particle. It has been shown [36–40] that the rms of stochastic charge fluctuations varies as $\delta\sqrt{\langle Q_d\rangle}$, where δ is a parameter depending on the plasma conditions and close to 0.5. Thus for mean charge around $-3e$ the charge distribution should lie mainly between $-1e$ and $-5e$. However, in our case we can expect a broader distribution, taking into account two reasons. First for small particles with a charge of about a few electrons the image force (polarizability) correction starts playing role; see [37]. And for electron temperature less then 0.1 eV the correction factor can be up to 3. That is a significantly broadened distribution, so dust particles can experience fluctuations to neutral and positive charges; see Fig. 9. Another reason for the broadened distribution could be the earlier freezing of the charge distribution so it remains the same while the mean charge decreases. Indeed as $t>t_d$ the charge is not in equilibrium with the surrounding plasma, so the existing charge distribution should remain unchanged or changed slightly during the later stages. Unfortunately, in this experiment the ratio between positively and negatively charged particles has not been measured due to experimental limitations concerned with the fact that dust grains do not stay in the laser sheet for a sufficiently long time due to their out-of-plane thermal motion. Thus to elaborate on the true reason for the presence of residual charges of different polarities one needs additional measurements of the charge distributions.

The considered decharging model predicts a higher residual charge for lower pressure. For low pressure the temperature relaxation time scale exceeds the plasma density decay time (see characteristic times for 0.4 mbar in Table II). This leads to a quick increase of the charging time and makes charge freezing at an early stage of decay keeping charge at a relatively high value. In fact larger charges were measured for the higher pressure. A possible explanation for

this is an electron reheating in late afterglow from metastable atoms [41]. The presence of a significant amount of argon metastables in PKE discharge have been established by plasma modeling [42] and by experimental measurements [43]. Due to reheating, the electrons can have temperatures a few times more than room temperature which will lead to an increase of the residual charge on dust particles. As reheating is more effective for high pressures, larger charges are thus expected.

VI. CONCLUSION

Residual dust-particle charges have been measured in the late afterglow of a dusty plasma. Dust particles have been grown directly in the plasma by sputtering of a polymer material previously deposited on electrodes. Dust particles with a radius of few hundreds of nanometers are levitating after the power of the discharge is switched off. The gravity was balanced by an upward thermophoretic force. Residual charges were determined from an analysis of dust oscillations, which were excited by applying a sinusoidal bias to the bottom electrode.

Positive, negative, and noncharged dust particles have been detected. The mean residual charge for 200-nm-radius particles was measured. The particle charge is about $-5e$ at a pressure of 1.2 mbar and about $-3e$ at a pressure of 0.4 mbar. A model for the dusty plasma decay was exploited to explain the experimental data. According to this model the dusty plasma decay occurs in four stages: temperature relaxation stage, density decay stage, dust-charge volume stage, and frozen stage (ice age IV). The main decrease of the dust charge happens during the first stage due to cooling of the electron gas. The final residual charge established during the third stage when the density of ions exceeds the density of electrons and the plasma density is still high enough to affect the charge. Measured values of the dust residual charges are in good agreement with values predicted by the model. However, the residual charge dependence on discharge conditions and the detection of positively charged particles show that a more detailed model taking into account various phenomena (electron reheating, electron release [44], afterglow chemistry) in decaying plasma has to be developed for a better understanding of dusty plasma afterglow.

ACKNOWLEDGMENTS

The authors would like to thank S. Dozias and B. Dumax for electronic support, J. Mathias for optical support, and Y. Tessier for experimental support. The PKE-Nefedov chamber has been made available by the Max-Planck-Institute for Extraterrestrial Physics, Germany, under the funding of DLR/BMBF under Grant No. 50WM9852. This work was supported by CNES under Contract No. 793/2000/CNES/8344. This work is partly supported by the French-Australian integrated research program (FAST) of the French foreign affairs ministry and the International Science Linkages established under the Australian Government's innovation statement, Backing Australia's Ability and University of Sydney Research and Development Scheme.

[1] A. P. Nefedov *et al.*, New J. Phys. **5**, 33.1 (2003).
[2] A. Bouchoule and L. Boufendi, Plasma Sources Sci. Technol. **2**, 204 (1993).
[3] M. Cavarroc, M. C. Jouanny, K. Radouane, M. Mikikian, and L. Boufendi, J. Appl. Phys. **99**, 064301 (2006).
[4] M. Mikikian, L. Boufendi, A. Bouchoule, H. M. Thomas, G. E. Morfill, A. P. Nefedov, V. E. Fortov, and the PKE-Nefedov team, New J. Phys. **5**, 19.1 (2003).
[5] M. Mikikian and L. Boufendi, Phys. Plasmas **11**, 3733 (2004).
[6] D. Samsonov and J. Goree, J. Vac. Sci. Technol. A **17**, 2835 (1999).
[7] A. A. Samarian and B. W. James, Phys. Lett. A **287**, 125 (2001).
[8] A. Bouchoule, *Dusty Plasmas: Physics, Chemistry and Technological Impacts in Plasma Processing* (Wiley, New York, 1999).
[9] I. A. Belov, A. S. Ivanov, D. A. Ivanov, A. F. Pal, A. N. Starostin, A. V. Filippov, A. V. Demyanov, and Y. V. Petrushevich, JETP **90**, 93 (2000).
[10] U. Konopka *et al.*, New J. Phys. **7**, 227 (2005).
[11] S. Vladimirov, K. Ostrikov, and A. Samarian, *Physics and Applications of Complex Plasmas* (Imperial Press, London, 2005).
[12] E. B. Tomme, D. A. Law, B. M. Annaratone, and J. E. Allen, Phys. Rev. Lett. **85**, 2518 (2000).
[13] C. Zafiu, A. Melzer, and A. Piel, Phys. Rev. E **63**, 066403 (2001).
[14] A. A. Samarian and S. V. Vladimirov, Phys. Rev. E **67**, 066404 (2003).
[15] O. S. Vaulina, A. A. Samarian, B. W. James, O. F. Petrov, and V. E. Fortov, JETP **96**, 1037 (2003).
[16] N. J. Prior, L. W. Mitchell, and A. A. Samarian, J. Phys. D **36**, 1249 (2003).
[17] S. Ratynskaia *et al.*, Phys. Rev. Lett. **93**, 085001 (2004).
[18] C. Arnas, M. Mikikian, and F. Doveil, Phys. Rev. E **60**, 7420 (1999).
[19] M. A. Childs and A. Gallagher, J. Appl. Phys. **87**, 1086 (2000).
[20] A. Ivlev *et al.*, Phys. Rev. Lett. **90**, 055003 (2003).
[21] H. Rothermel, T. Hagl, G. E. Morfill, M. H. Thoma, and H. M. Thomas, Phys. Rev. Lett. **89**, 175001 (2002).
[22] P. Shukla and A. Mamun, *Introduction to Dusty Plasma Physics* (IOP, Bristol, 2002).
[23] F. Zheng, Adv. Colloid Interface Sci. **97**, 255 (2002).
[24] R. N. Varney, Phys. Rev. **88**, 362 (1952).
[25] Z. Li and H. Wang, Phys. Rev. E **70**, 021205 (2004).
[26] I. Goldhirsch and D. Ronis, Phys. Rev. A **27**, 1616 (1983).
[27] I. Goldhirsch and D. Ronis, Phys. Rev. A **27**, 1635 (1983).
[28] L. Waldmann, Z. Naturforsch. A **14**, 589 (1959).
[29] K. DeBleecker, A. Bogaerts, and W. Goedheer, Phys. Rev. E

71, 066405 (2005).
[30] W. Li and E. J. Davis, J. Aerosol Sci. **26**, 1063 (1995).
[31] W. Li and E. J. Davis, J. Aerosol Sci. **26**, 1085 (1995).
[32] M. A. Gallis, D. J. Rader, and J. R. Torczynski, Aerosol Sci. Technol. **36**, 1099 (2002).
[33] L. Landau and E. Lifchitz, *Physique Théorique* (Édition Mir Moscou, 1982), Vol. 1.
[34] Y. P. Raizer, *Gas Disharge Physics* (Springer, Berlin, 1991).
[35] V. N. Tsytovich, Phys. Usp. **40**, 53 (1997).
[36] T. Matsoukas and M. Russell, J. Appl. Phys. **77**, 4285 (1995).
[37] T. Matsoukas, M. Russell, and M. Smith, J. Vac. Sci. Technol. A **14**, 624 (1996).
[38] O. S. Vaulina, S. A. Khrapak, A. P. Nefedov, and O. F. Petrov, Phys. Rev. E **60**, 5959 (1999).
[39] S. A. Khrapak, A. P. Nefedov, O. F. Petrov, and O. S. Vaulina, Phys. Rev. E **59**, 6017 (1999).
[40] C. Cui and J. Goree, IEEE Trans. Plasma Sci. **22**, 151 (1994).
[41] G. Wenig, M. Schulze, P. Awakowicz, and A. v. Keudell, Plasma Sources Sci. Technol. **15**, S35 (2006).
[42] M. R. Akdim and W. J. Goedheer, Phys. Rev. E **67**, 066407 (2003).
[43] M. Mikikian, L. Boufendi, and A. Bouchoule, in *Proceedings of the 30th EPS Conference on Controlled Fusion and Plasma Physics, St Petersburg, 2003*, edited by R. Koch and S. Lebedev, vol. 27A of *ECA* (European Physical Society, Paris, 2003), pp. O-3.1B.
[44] J. Berndt, E. Kovacevic, V. Selenin, I. Stefanovic, and J. Winter, Plasma Sources Sci. Technol. **15**, 18 (2006).